Long-Range RNA-RNA Interactions Circularize the Dengue Virus Genome

Diego E. Alvarez,[1] María F. Lodeiro,[1] Silvio J. Ludueña,[2] Lía I. Pietrasanta,[2]
and Andrea V. Gamarnik[1]*

*Fundación Instituto Leloir, Avenida Patricias Argentinas 435, Buenos Aires 1405, Argentina,[1] and
Centro de Microscopías Avanzadas, Facultad de Ciencias Exactas y Naturales, Pabellón I,
Universidad de Buenos Aires, Buenos Aires, Argentina[2]*

Secondary and tertiary RNA structures present in viral RNA genomes play essential regulatory roles during translation, RNA replication, and assembly of new viral particles. In the case of flaviviruses, RNA-RNA interactions between the 5′ and 3′ ends of the genome have been proposed to be required for RNA replication. We found that two RNA elements present at the ends of the dengue virus genome interact in vitro with high affinity. Visualization of individual molecules by atomic force microscopy reveled that physical interaction between these RNA elements results in cyclization of the viral RNA. Using RNA binding assays, we found that the putative cyclization sequences, known as 5′ and 3′ CS, present in all mosquito-borne flaviviruses, were necessary but not sufficient for RNA-RNA interaction. Additional sequences present at the 5′ and 3′ untranslated regions of the viral RNA were also required for RNA-RNA complex formation. We named these sequences 5′ and 3′ UAR (upstream AUG region). In order to investigate the functional role of 5′-3′ UAR complementarity, these sequences were mutated either separately, to destroy base pairing, or simultaneously, to restore complementarity in the context of full-length dengue virus RNA. Nonviable viruses were recovered after transfection of dengue virus RNA carrying mutations either at the 5′ or 3′ UAR, while the RNA containing the compensatory mutations was able to replicate. Since sequence complementarity between the ends of the genome is required for dengue virus viability, we propose that cyclization of the RNA is a required conformation for viral replication.

Outbreaks and epidemics caused by dengue virus continue to pose a public health problem in tropical and subtropical regions (60). It is estimated that more than 50 million human infections occur annually, and 2.5 billion people are at risk of dengue virus infection worldwide. Despite the wide morbidity and mortality associated with dengue virus infections, the molecular biology of this virus is not well understood, and at present, neither specific antiviral therapy nor licensed vaccine exists. Thus, defining the molecular determinants that regulate utilization of the viral RNA in the infected cell is of central importance for understanding the dengue virus life cycle.

The genomes of positive-strand RNA viruses participate in at least three different processes in the cytoplasm of the infected host cell: they serve as mRNA to direct the synthesis of viral proteins, they act as a template for genome amplification, and they are packaged along with structural proteins during viral assembly. The molecular mechanisms controlling the utilization of the viral RNA in each step of the viral life cycle are still poorly understood. Several lines of evidence support the notion that viral RNA genomes could circularize to regulate initiation of translation and RNA synthesis at the 5′ and 3′ ends of the genome (4, 15, 18, 22, 23, 30, 31, 33, 38, 44). However, the molecular nature of 5′-3′ associations and the details of how different conformations of the RNA participate in the viral replication pathways remain unclear.

Different strategies for 5′-3′-end contact in the genome of positive-strand RNA viruses were proposed to be mediated by RNA binding proteins. Viral RNAs bearing a 5′-cap structure (m7GpppN) and a 3′ poly(A) tail could circularize by a protein bridge between eIF4G and eIF4E from the cap-binding complex and the poly(A) binding protein (PABP) similar to that observed for cellular mRNAs (59). Other strategies were proposed for viruses lacking the cap structure and/or the poly(A) tail. For instance, picornaviruses do not have a cap at the 5′ end but instead use a highly structured 5′ untranslated region (UTR) to bind the cellular poly(C) binding protein which mediates the interaction with PABP and the viral poly(A) tail (18, 30, 56). The viral protein NSP3 is a candidate to mediate interactions between the ends of the rotavirus genome. This protein binds the 3′ end of the viral RNA and the cellular protein IF4G of the cap-binding complex (46, 54). In the case of viral bovine diarrhea virus, which lacks both the cap structure and the poly(A) tail, binding of NFAR proteins to the viral 5′ and 3′ UTRs was found to mediate contacts between the 5′ and 3′ ends of the RNA (33). A different strategy was postulated for circularization of flavivirus genomes. In this case, direct RNA-RNA interactions between sequences present at the 5′ and 3′ ends of the viral genome have been proposed (23, 37, 38, 62). For all-mosquito borne flaviviruses, within the 3′ UTR, there is a putative cyclization sequence (CS) (3′ CS), which is complementary to a sequence located in the capsid coding region near the 5′ end of the genome (5′ CS) (11, 23, 38, 51).

The genus flavivirus of the *Flaviviridae* family includes important human pathogens such as dengue virus, yellow fever

---

* Corresponding author. Mailing address: Fundación Instituto Leloir, Avenida Patricias Argentinas 435, Buenos Aires 1405, Argentina. Phone: 54-11-5238-7500. Fax: 54-11-5238-7501. E-mail: agamarnik @leloir.org.ar.

virus, West Nile virus, and Japanese encephalitis virus. As with other positive-strand RNA viruses, replication of flaviviruses proceeds along a two-step pathway in the host cell. After synthesis and maturation, the nonstructural proteins and the viral RNA form a replication complex that catalyzes the synthesis of the negative-strand RNA, which in turn is used as a template to amplify new strands of genomic RNA. Even though contacts between the ends of the genomes of positive-strand RNA viruses have not been directly demonstrated, for flaviviruses, there is functional evidence supporting the hypothesis that genome circularization is required for viral replication (38). The single-stranded RNA genome of flaviviruses is about 11 kb long and encodes one open reading frame flanked by 5′ and 3′ UTRs of about 100 and 600 nucleotides, respectively (49). The highly structured 3′ UTR ends in a very conserved 3′ stem-loop (SL), which is absolutely required for viral replication (8, 42, 47, 48, 64). The structure of the 3′ SL is preceded by the putative cyclization sequence 3′ CS. There is a total of 11 or 12 contiguous base pairings possible between 5′ and 3′ CS of West Nile, dengue, Japanese encephalitis, and Murray Valley virus RNAs (for a review, see reference 41) and 18 nucleotides in the case of yellow fever RNA (11). Computer analysis using the complete RNA of Kunjin virus indicates that base pairing of 5′-3′ CS is thermodynamically feasible (37). Using in vitro assays, it has been demonstrated that efficient RNA synthesis by dengue virus RNA-dependent RNA polymerase requires both the 5′ and 3′ CS (62). Interestingly, Khromykh et al. examined the importance of 5′ and 3′ CS complementarity using mutated Kunjin virus replicons (38). Specific mutations in 5′ or 3′ CS abolished RNA amplification, while reconstitution of the base pairing with foreign sequences restored viral replication, suggesting a functional role for 5′-3′-end contact in the viral genome.

In this article, we show that the dengue virus genome circularizes through RNA-RNA interactions in the absence of proteins. Using atomic force microscopy (AFM), we visualized individual dengue virus RNA molecules in circular conformations. We found that sequences encompassing the previously reported 5′ and 3′ CS regions are essential but not sufficient for RNA interactions. We identified a new element of 16 nucleotides present at the 5′ and 3′ UTRs as an important determinant for RNA-RNA association. Importantly, functional studies obtained here with recombinant dengue viruses strongly suggest that RNA complementarity between the ends of the genome is necessary for viral viability.

MATERIALS AND METHODS

RNA preparation. RNAs were obtained by in vitro transcription using T7 RNA polymerase (90 min, 37°C) and treated with DNase I RNase-free to remove templates. The RNAs were purified using an RNeasy Mini kit (QIAGEN Inc.) to remove free nucleotides and quantified spectrophotometrically, and their integrity was verified by electrophoresis on agarose gels. All numbers given below in parentheses refer to nucleotide positions of a dengue virus type 2 strain 16681 infectious cDNA clone (GenBank accession number U87411).

The sequences corresponding to the 5′ UTR-C62 (nucleotides [nt] 1 to 160) and 3′ SL (nt 10617 to 10723) were amplified by PCR from a dengue virus infectious clone (40) with a forward primer carrying the T7 RNA polymerase promoter. Mutations in 5′ CS (mutations 143, 144, 145, and 146) were introduced by PCR using antisense primers carrying the desired mutation. Mutations in the 5′ upstream AUG region (UAR) (mutations 131, 133, 139, 170, and 175) and mutant 3′ SL 177 were generated by overlapping PCR. These PCR products

were directly used as templates for in vitro transcription. The position and the specific nucleotide substitution are indicated in Fig. 4, 6, and 7, respectively.

To generate the model RNA molecule of 2.3 kb, pGL5′3′DV plasmid was constructed by introducing the 5′ UTR-C62 (nt 1 to 160) into pGL3-Basic vector (Promega) between SacI and NcoI restriction sites and dengue virus 3′ UTR (nt 10269 to 10723) between XbaI and BamHI sites. The construct carrying dengue virus 5′ UTR-C62 and 3′ UTR flanking luciferase coding sequence was amplified by PCR, and the product was used as a template for in vitro transcription. Deletions of 96 nucleotides (nt 10627 to 10723, deleting the 3′ UAR) and 106 nucleotides (nt 10617 to 10723, deleting both the 3′ CS and UAR) at the 3′ end were introduced into the construct by PCR using pGL5′3′DV as a template. The DNA template for antisense RNA synthesis was generated by PCR amplification of 1.6-kb or 1-kb fragments of luciferase sequence. Full-length dengue virus RNA was generated using as a template dengue virus type 2 strain 16681 infectious cDNA clone (pD2/IC-30P-A) linearized by the XbaI restriction enzyme. A DNA template to synthesize an antisense RNA molecule spanning NS4B and NS5 coding sequence (nt 6970 to 10721) was also generated by PCR.

RNA binding assays. RNA-RNA interactions were analyzed by electrophoretic mobility shift assays. Uniformly ^{32}P-labeled RNA probes were obtained by in vitro transcription using T7 RNA polymerase and purified on 5% polyacrylamide gels and 6 M urea. The binding reaction mixtures contained 5 mM HEPES, pH 7.9, 100 mM KCl, 5 mM MgCl$_2$, 3.8% glycerol, 2.5 μg tRNA, 5′ UTR-C62 (concentration indicated in each case), and uniformly ^{32}P-labeled 3′ SL RNA (0.1 nM, 30,000 cpm), in a final volume of 30 μl. RNA samples were heat denatured at 85°C for 5 min and slow cooled to room temperature. RNA-RNA complexes were analyzed by electrophoresis through native 5% polyacrylamide gels supplemented with 5% glycerol. Gels were prerun for 30 min at 4°C at 150V, and then 25 μl of sample was loaded and electrophoresis was allowed to proceed for 4 h at constant voltage. Gels were dried and visualized by autoradiography or exposed on a PhosphorImager plate.

To determine relative binding affinities, radiolabeled 3′ SL (0.1 nM) was titrated with increasing concentrations of the unlabeled RNA as indicated in each case. The total radioactivity for each lane was determined by quantifying the radioactivity incorporated into the RNA-RNA complex plus the amount remaining in the free probe. For each case, we calculated the fraction bound, θ. The apparent K_ds were estimated by fitting the data using nonlinear regression analysis as follows: θ = [RNA]/([RNA] + K_d). Because the bound RNA was incorporated into two bands, we considered bound RNA as a single species equal to the sum of both bands.

AFM sample preparation and imaging. For AFM imaging, sense and antisense RNA molecules were denatured by heating to 85°C for 1 min and slow cooled to room temperature to form double-stranded RNA species in buffer A containing 20 mM HEPES, pH 8, and 4 mM MgCl$_2$. Samples were diluted to 1 ng/μl in buffer A, and 20 μl of the mix was deposited onto freshly cleaved muscovite mica. After 2 to 5 min, the sample was gently washed with 0.5 ml milliQ water to remove molecules that were not firmly attached to the mica and blown dry with nitrogen. Tapping-mode AFM was performed using a Nanoscope III Multimode-AFM (Digital Instruments, Veeco Metrology, Santa Barbara, CA) with a J-type piezoelectric scanner with a maximal lateral range of 120 μm. Microfabricated silicon cantilevers of 125 μm in length and a force constant of ~40 N m^{-1} were used (NanoDevices, Veeco Metrology, Santa Barbara, CA). Cantilever oscillation frequency was tuned to the resonance frequency of the cantilever (280 to 350 kHz). After a period of 15 to 30 min of thermal relaxation, initial engagement of the tip was achieved at scan size zero to minimize sample deformation and tip contamination. The images (512 by 512 pixels) were captured with a scan size of between 0.5 and 3 μm at a scan rate of 1 to 2 scan lines per s. Images were processed by flattering using Nanoscope software (Digital Instruments) to remove background slope. Measurements were done using Nanoscope software and ImageJ, version 1.3 (NIH).

Construction of recombinant dengue viruses. The full-length cDNA of dengue virus type 2 pD2IC/30P-A was modified by site-directed mutagenesis to generate a 3′ UTR cassette between unique AflII and XbaI restriction sites. To this end, PCR product generated with sense primer AVG-62 (5′-CACCAATGTTGAGA CATAGCATTGA-3′) and antisense primer AVG-91 (5′-GTTTCATCTTAAG TTTTGCTTTCTA-3′) and the product of a second PCR obtained with the sense primer AVG-90 (5′-TAGAAAGCAAAACTTAAGATGAAAC-3′) and antisense primer AVG-63 (5′-ACTGGTGAGTACTCAACCAAGTCAT-3′) were fused by overlapping PCR. This PCR product was cloned into pGEM-T Easy (Promega), generating pGEM-3′UTR*AflII*. The AvrII-ClaI fragment of pD2IC/30P-A was replaced with the AvrII-ClaI fragment of pGEM-3′UTR*AflII* to generate pD2/IC*AflII*. The mutant DV-3′UAR 177 was obtained by exchanging the wild-type fragment of AflII-XbaI with the fragment containing the mutation 10634-CA_C_AGAUC_G_UGCUGU_G_U and a G/C substitution at position 10718

(nucleotide substitutions are underlined). The mutant DV-5′UAR 175, containing the mutation 80-ACAAGACACAUCUGUG, was obtained by overlapping PCR using a 1,508-nucleotide-long fragment from the 5′ end of pD2/ICAflII. The PCR fragment was digested with SacI and SphI, and the resulting fragment was cloned into the homologous restriction sites within pD2/ICAflII or the DV-3′UAR 177 mutant clone to obtain DV-5′UAR 175 and DV-5′3′UAR 175-177 cDNAs, respectively.

RNA transfection and recovery of viruses. Wild-type (WT) or recombinant plasmid DNAs were linearized with XbaI and used as templates for transcription by T7 RNA polymerase in the presence of m^7GpppA cap structure analog. RNA transcripts (3 μg) were transfected with Lipofectamine 2000 (Invitrogen) into BHK-21 cells grown in 60-mm-diameter tissue culture dishes. The transfected cells were trypsinized on day 3 posttransfection and two-thirds of the total cells were reseeded. This procedure was repeated every 3 days for 21 days. Supernatants derived from transfected BHK-21 cells were harvested at 3, 6, 9, 12, 15, 18, and 21 days posttransfection and used to search for infectious dengue virus. For plaque assays, 3.0×10^4 to 4.0×10^4 BHK-21 cells were seeded per well in 24-well plates and allowed to attach overnight. Transfected cell supernatants were serially diluted, and 0.1 ml of the inoculum was incubated on the cells for 60 min. Afterwards, 1 ml of overlay (1× minimal essential alpha medium, 2% NCS, 100 U of penicillin/ml, 100 μg of streptomycin/ml, and 0.8% methyl cellulose) was added to each well. Cells were fixed 7 to 9 days postinfection with 10% formaldehyde and stained with crystal violet.

Immunofluorescence. Transfected cells with wild-type and mutated full-length dengue virus RNA were used for immunofluorescence assay (IFA). BHK-21 cells were grown in 60-mm-diameter tissue culture dishes containing a 1-cm² coverslip inside. The coverslips were removed and directly used for IFA analysis. The transfected cells were trypsinized at day 3, and two-thirds of the total cells were reseeded to a 60-mm-diameter tissue culture dish containing a new coverslip inside. This procedure was repeated every 3 days for 21 days. At each time point, a 1:200 dilution of murine hyperimmune ascitic fluid against dengue virus type 2 in phosphate-buffered saline–0.2% gelatin was used to detect viral antigens. Cells were fixed in paraformaldehyde. Alexa Fluor 488 rabbit anti-mouse immunoglobulin G and Alexa Fluor 488 goat anti-rabbit immunoglobulin G conjugates (Molecular Probes) were used as detector antibodies at a 1:500 dilution. Photomicrographs (×200 magnification) were acquired with an Olympus BX60 microscope coupled to a CoolSnap-Pro digital camera (Media Cybernetics) and analyzed with Image-Pro Plus software.

Viral RNA extraction and sequencing. Viral RNA was TRIZOL extracted from a 200-μl aliquot of the media from transfected cells. Dengue virus RNA was reverse transcribed and amplified. Primers in the reverse transcriptase PCR (RT-PCR) were targeted to amplify nt 1 to 1451 in the 5′ end and nt 10201 to 10723 in the 3′ end. This primer design excluded the last 23 nt of the genome from the sequencing analysis. The RT-PCR products were sequenced using an ABI 377 automated DNA sequencer and Big Dye terminator chemistry (Applied Biosystems).

RESULTS

Specific RNA-RNA interactions in the dengue virus genome. To investigate RNA-RNA association between different RNA elements of the dengue virus genome, we developed a method to examine the interaction of in vitro-generated RNA molecules using gel shift assays. For this purpose, radiolabeled RNAs corresponding to each of the four domains of dengue virus 3′ UTR (variable region, A2, A3, and 3′ SL [Fig. 1A]) were in vitro transcribed. We evaluated the interaction of an RNA molecule corresponding to the 98-nucleotide-long 5′ UTR followed by 60 nucleotides of the coding region of the C protein (named here 5′UTR-C62 RNA) (Fig. 1A) with each of the four RNA probes. The RNAs were heat denatured, mixed, cooled to room temperature to allow folding, and used in gel shift assays. RNA-RNA complexes were observed only when the 5′UTR-C62 RNA was incubated with the RNA probe corresponding to the last 106 nucleotides of the viral genome (3′ SL RNA). RNA titrations indicate high affinity between the two RNA elements with an apparent dissociation constant (K_d) of 8 nM (Fig. 1B).
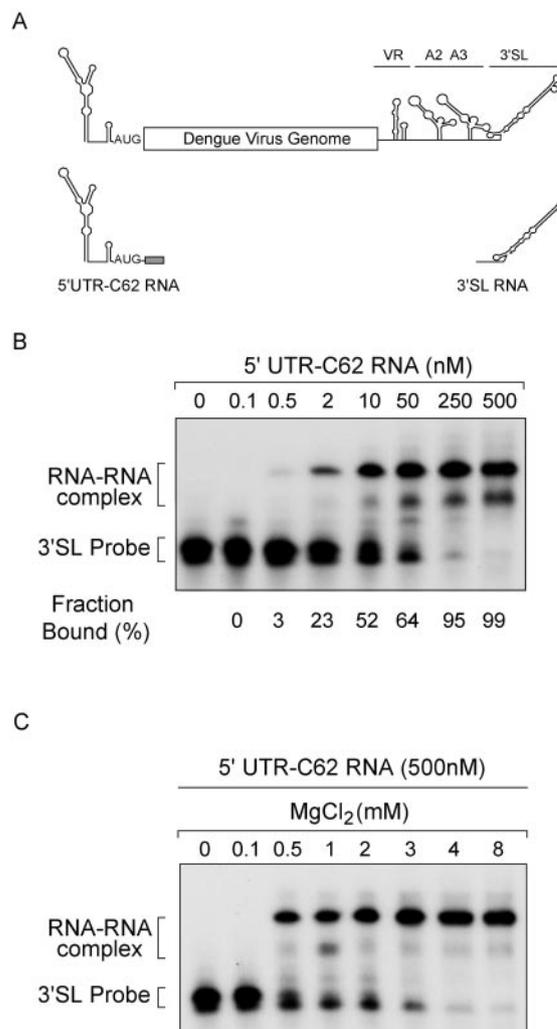

FIG. 1. Biochemical assays reveal RNA-RNA complex formation between the end sequences of dengue virus RNA. (A) Schematic representation of the dengue virus genome showing the predicted secondary structures at the 5′ and 3′ UTR. The four domains of the 3′ UTR, variable region (VR), A2, A3, and 3′ stem-loop (3′ SL), are indicated. The schematic representation of RNA molecules used for binding assays, 5′ UTR-C62 and 3′ SL, are also shown. (B) Mobility shift assays showing RNA-RNA associations. Uniformly labeled 3′ SL RNA, corresponding to the last 106 nucleotides of dengue virus type 2, was incubated with increasing concentrations of the 5′ UTR-C62 RNA corresponding to the first 160 nucleotides of the viral genome. The 5′ UTR-C62 RNA was used from 0 to 500 nM as indicated on the top of the gel. The locations of the 3′ SL probe (Probe) and the RNA-RNA complex are shown. Quantification of the fraction of probe bound for each concentration of the RNA is also indicated at the bottom of the gel. (C) RNA-RNA complex is formed only in the presence of Mg^{2+}. The 3′ SL probe was incubated with an excess of the 5′ UTR-C62 RNA (500 nM), and complex formation was examined in the presence of increasing concentrations of Mg^{2+}, from 0 to 8 mM.

To determine specificity of the detected RNA-RNA complex, we measured the efficiency of complex formation in the presence of various amounts of tRNA or unrelated RNA (up to a 1,000-fold molar excess with respect to the unlabeled 5′ UTR-C62 RNA) at different ionic strengths (up to 500 mM KCl). Under these conditions, the RNA complex remained
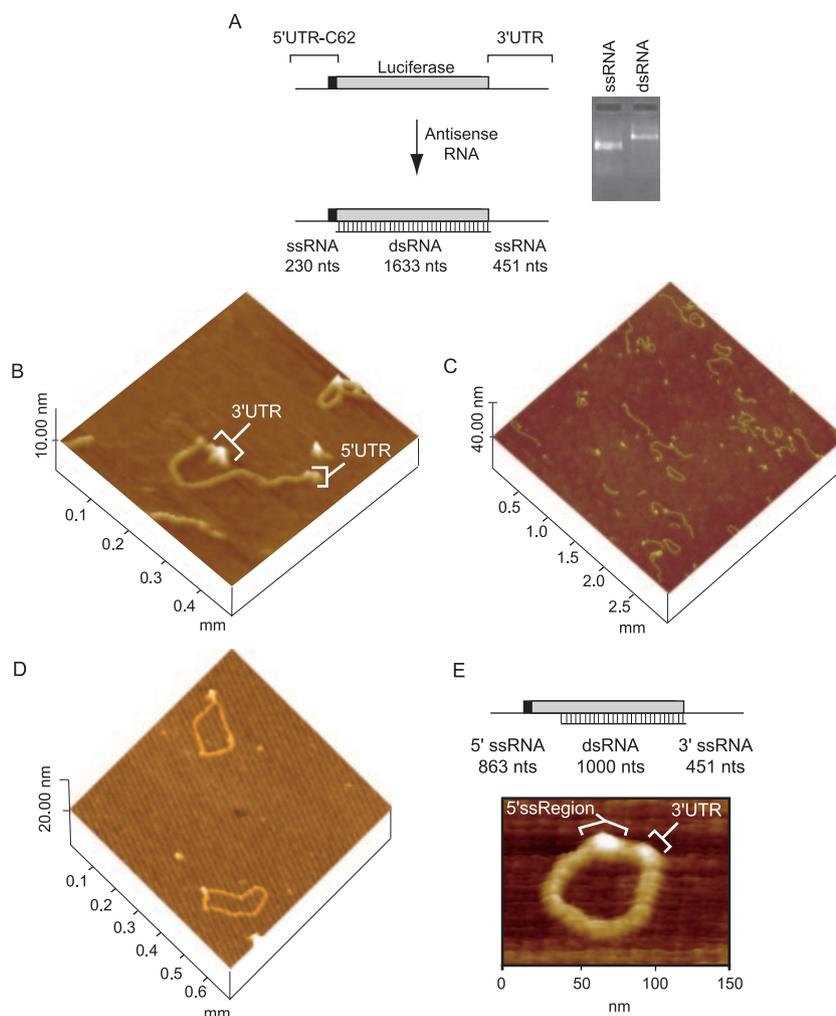
FIG. 2. Single-molecule analysis reveals cyclization of an RNA molecule carrying the 5′- and 3′-end sequences of dengue virus. (A) Schematic representation of a model RNA molecule of 2.3 kb showing the 5′ and 3′ dengue virus sequences flanking the luciferase coding sequence. Annealing of an antisense RNA of 1,633 nucleotides is shown. The resulting molecule bears single-stranded overhangs in the 5′ and 3′ ends of 230 and 451 nucleotides, respectively. On the right, purified single-stranded RNA (ssRNA) and double-stranded RNA were resolved on a 1% agarose gel and visualized by ethidium bromide staining. (B) Visualization of the model RNA molecules by AFM. A single RNA molecule is shown in a linear conformation. The double-stranded RNA region is flanked by single-stranded regions corresponding to the 5′ UTR-C62 and 3′ UTR of dengue virus. (C) An image of a representative field of RNA molecules deposited on mica obtained by tapping-mode AFM. Circular, linear, and head-to-tail dimers were observed. (D) Image of individual RNA molecules in circular conformation. Contacts between the 5′ and 3′ single-stranded regions of the molecules can be observed. (E) Schematic representation of the same RNA molecule shown in A hybridized with an antisense RNA molecule of 1 kb. The double-stranded region of 1 kb is flanked by a 5′ single-stranded region of 863 nucleotides that contained the 160 nucleotides of the 5′ end of dengue virus and a 3′ single-stranded region that corresponds to the 3′ UTR of dengue virus. At the bottom, a representative image of an individual molecule with a double-stranded region of 1 kb is shown in circular conformation.

unchanged, and it was chased only by specific unlabeled 3′ SL RNA (data not shown). Divalent cations are known to favor RNA tertiary structures under physiological ionic strengths (14, 43). Thus, we analyzed the effect of different concentrations of $MgCl_2$ and $NiCl_2$ on complex formation. We observed an absolute requirement of Mg^{2+} for RNA-RNA interaction (Fig. 1C). Mg^{2+} could not be replaced by Ni^{2+}; in fact, in the presence of Ni^{2+}, complex formation was reduced. In the presence of 100 mM KCl, 4 mM Mg^{2+} was required to allow 100% of the complex to be formed, suggesting that tertiary structures in the RNA are necessary for 5′ UTR-C62–3′ SL interaction. Taking these data together, by using in vitro RNA binding

assays, it was possible to identify direct and specific RNA-RNA interactions between the 3′ SL and the 5′ UTR-C62 RNA.

Atomic force microscopy reveals circularization of dengue virus RNA. To examine whether the RNA-RNA interaction observed in gel shift assays was sufficient for mediating long-range interactions leading to single RNA molecule circularization, we used AFM (25). This technique allows visualization of individual molecules in physiological environments. In agreement with previous reports, single-stranded RNA molecules acquired compact conformations precluding visualization of intramolecular interactions (27, 36). In order to obtain RNA molecules suitable for AFM analysis, we used a method that

TABLE 1. Quantification of different conformations of RNA molecules visualized by AFM

Conformation	No. of molecules[a]	% of molecules
Total	200	100
Circular	90	45
Linear	84	42
Head-to-tail	26	13
RNA Δ3′SL CS		
linear	200	100

[a] Molecules were counted only when the apparent contour length of the double-stranded region was 437 ± 10 nm.

was previously employed to visualize conformations of cellular mRNAs (59). This method consists of generating double-stranded RNA regions in the center of the molecule, leaving the sequences presumably involved in long-range interactions as single-stranded overhangs. Based on this report, we first developed a model RNA molecule of 2.3 kb carrying the 5′ UTR-C62 and the complete 3′ UTR of dengue virus flanking a luciferase coding sequence and a second RNA molecule of 1.6 kb complementary to the luciferase coding region. Hybridization of these two RNA molecules leaves the 5′ and 3′ dengue virus sequences of interest as single-stranded overhangs (Fig. 2A). The sense and antisense RNA molecules were in vitro synthesized, treated with DNases, purified, and mixed after thermal denaturation. Annealing of the two RNAs and integrity of the molecules were confirmed by agarose gels (Fig. 2A). The samples were deposited onto freshly cleaved mica and analyzed using tapping-mode AFM in air. High-resolution images of individual molecules were used to measure contour lengths of the double-stranded region as well as the apparent volumes of the 5′ and 3′ overhang regions. The contour length of the 1,633-nt double-stranded region was 437 ± 3.5 nm with a rise per base pair of 0.27 nm. This observation is in good agreement with the values obtained for duplex RNA in the A form (50) and previous AFM data (7, 29). The single-stranded regions corresponding to the 5′ and 3′ UTR of dengue virus adopted globule-like conformations with apparent volumes of 25.7 ± 4.2 nm^3 and 131.4 ± 3.9 nm^3, respectively (Fig. 2B). Image analysis revealed the presence of both circular and linear conformations of the RNA. In Fig. 2C, we show a representative field (3 μm by 3 μm) containing molecules in different conformations, and Fig. 2D shows a higher-resolution image (0.7 μm by 0.7 μm) depicting circular conformations of the RNA. The molecules were categorized as being either circular or linear by visual inspection of a series of images from more than six independent experiments in which only intact molecules, determined by size, were counted. We estimated that 45% of the intact molecules were circular, and the remainder were linear (Table 1). At the concentration used for imaging (1 ng of RNA/μl), about 13% of the molecules were observed as RNA-RNA head-to-tail dimers. As a control, an RNA molecule with a deletion of the last 106 nucleotides (Δ3′SL RNA) was constructed, annealed with the 1.6-kb antisense RNA, and used for AFM imaging analysis. Visual inspection of this RNA revealed the absence of molecules in circular conformation (Table 1). Taken together, these obser-
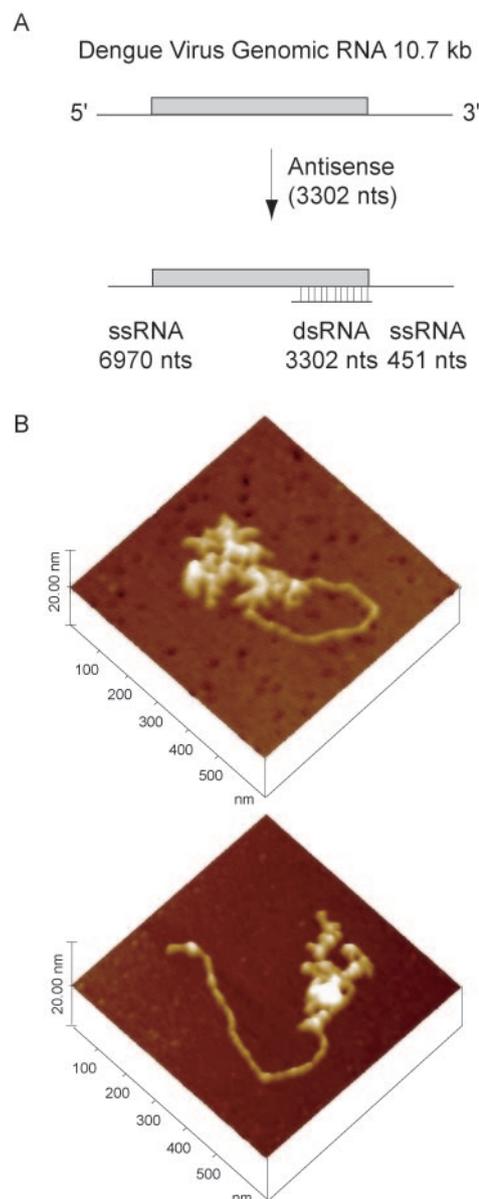

FIG. 3. Visualization of genome-length dengue virus RNA by AFM. (A) Schematic representation of the dengue virus genome. An antisense RNA anneals to the molecule, resulting in a 3,302-bp double-strand species with single-stranded regions of 6,970 and 451 nucleotides at the 5′ and 3′ ends, respectively. (B) Visualization of representative images of individual genome-length RNA molecules obtained by tapping-mode AFM.

vations indicate that long-range RNA-RNA contacts mediated by dengue virus sequences are capable of circularizing a model molecule. In addition, we confirmed that the last 106 nucleotides of the 3′ UTR are involved in RNA-RNA interaction, in agreement with the results obtained using RNA binding assays.

In these experiments, we were concerned about the possibility that the stiffness of the duplex RNA used in our model molecule could restrict RNA bending and circularization. Previous physicochemical studies performed with double-strand RNA polymers indicated that the persistence length (measure-
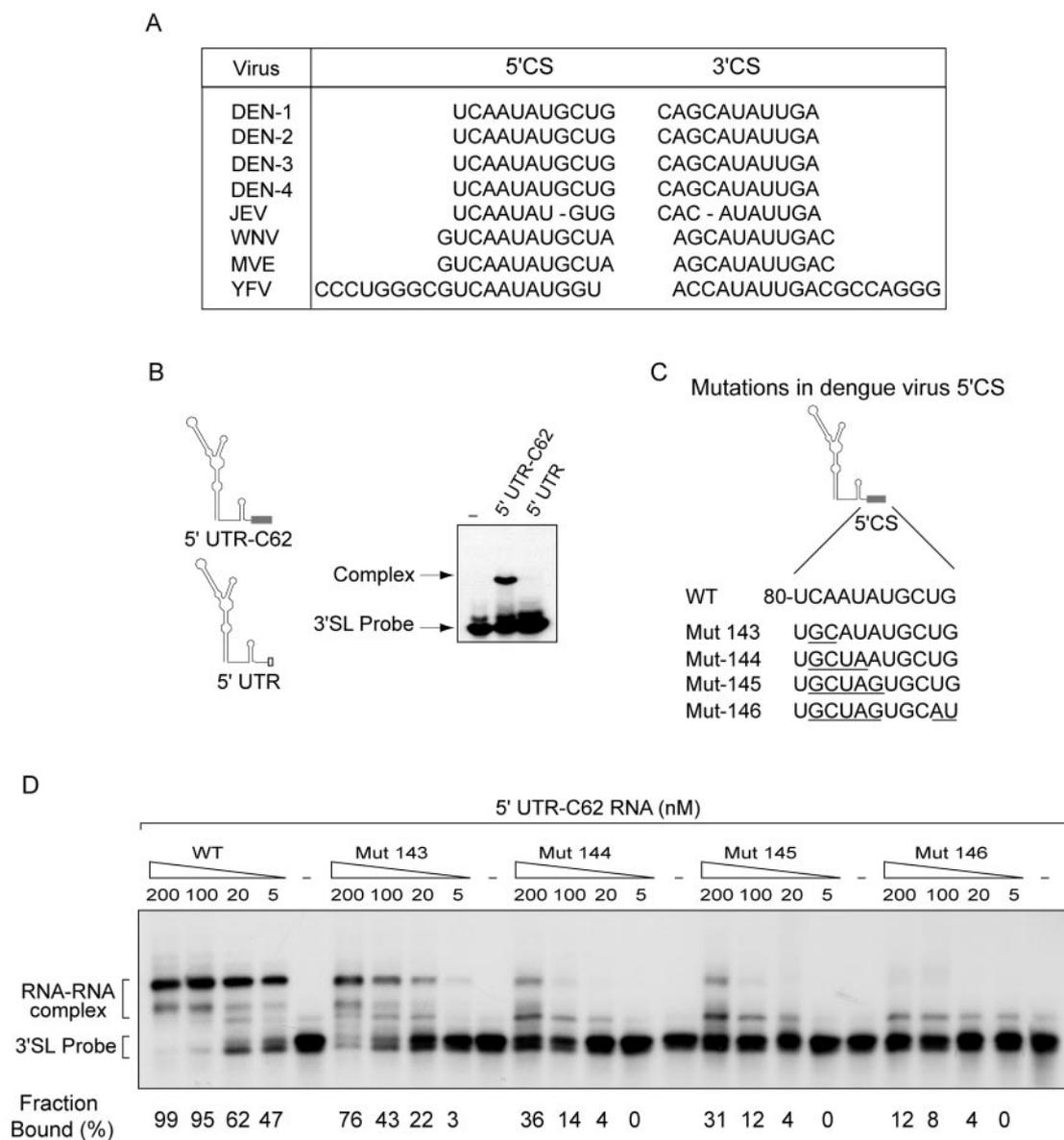
A

Virus	5'CS	3'CS
DEN-1	UCAAUAUGCUG	CAGCAUAUUGA
DEN-2	UCAAUAUGCUG	CAGCAUAUUGA
DEN-3	UCAAUAUGCUG	CAGCAUAUUGA
DEN-4	UCAAUAUGCUG	CAGCAUAUUGA
JEV	UCAAUAU -GUG	CAC - AUAUUGA
WNV	GUCAAUAUGCUA	AGCAUAUUGAC
MVE	GUCAAUAUGCUA	AGCAUAUUGAC
YFV	CCCUGGGCGUCAAUAUGGU	ACCAUAUUGACGCCAGGG

FIG. 4. Interaction between the 5′ and 3′ CS is required for RNA-RNA complex formation. (A) The nucleotide sequence of the 5′ and 3′ CS is conserved among different mosquito-borne flaviviruses (DEN, dengue virus; JEV, Japanese encephalitis virus; WNV, West Nile virus; MVE, Murray Valley encephalitis virus; and YFV, yellow fever virus). (B) On the left, a schematic representation of the two RNA molecules used, 5′ UTR-C62 and the RNA with a deletion of the 5′ CS (5′ UTR), is shown. On the right, mobility shift assay of the 3′ SL probe in the presence of 5′ UTR-C62 or 5′ UTR RNAs is shown. (C) Nucleotide sequences of the wild type and mutated 5′ CS are indicated. Underlined letters indicate the specific substitutions in mutants 143, 144, 145, and 146. (D) RNA mobility shift analysis showing the effect of mutations within the 5′ CS in the 5′ UTR-C62 RNA on binding to the 3′ SL RNA. Uniformly labeled 3′ SL RNA was incubated with increasing concentrations of wild-type and mutated 5′ UTR-C62 RNAs as indicated at the top of the gel. The mobility of the 3′ SL probe and the RNA-RNA complex is indicated on the left. Quantification of the fraction of probe bound for each concentration of the WT and mutated RNAs is also indicated at the bottom of the gel.

ment of the flexibility of the molecules) was around 110 nm (35) and that the optimal loop size was three to four times the persistence length (330 to 440 nm) (34, 61). The double-stranded region used in our model molecule was 437 nm, which is around the optimal size to allow free movement of the ends of the molecule. Therefore, we conclude that the stiffness of the double-stranded region in the RNA molecules used in our experiments should not be a limitation for RNA circulariza-tion. To better characterize the system, we designed various

antisense molecules that would leave single-stranded overhang regions of different lengths. All the molecules used (antisense from 1.6 to 1 kb) yielded similar results. Figure 2E shows the image of a representative molecule in a circular conformation with a double-stranded region of 1 kb.

Having shown that specific interactions between the 5′ and 3′ ends of dengue virus are capable of circularizing a model RNA molecule, we sought to analyze the conformation of the full-length dengue virus RNA. To this end, we in vitro synthe-
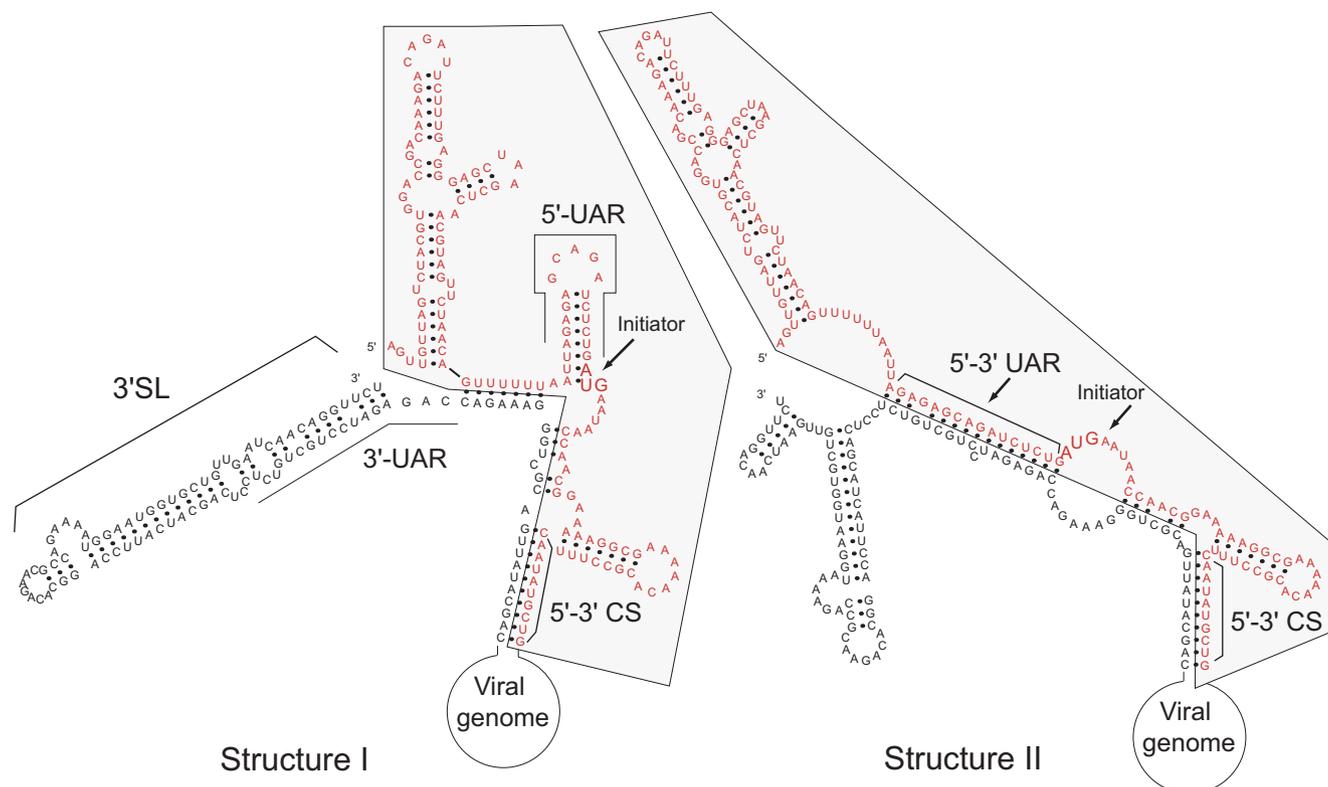
FIG. 5. Computer-generated secondary structures of the last 106 nucleotides (letters in black) and the first 143 nucleotides (letters in red) of dengue virus genomic RNA (65). The rest of the viral genome is represented schematically linking the 5′ and 3′ ends of the molecule. The predicted secondary structures I and II are those with the lowest ΔG (−90 and −91 kcal mol^{-1}, respectively). The conserved sequences 5′-3′ CS and 5′-3′ UAR and the 3′ SL are shown. The initiator AUG codon is indicated with arrows.

sized the 10.7-kb dengue virus RNA from a cDNA clone (40) and used it for AFM analysis. In order to visualize specific intramolecular interactions, we used a partially double-stranded RNA as described above. In this case, we designed an RNA molecule complementary to nucleotides 6971 to 10272 of dengue virus type 2, corresponding to the coding sequence of NS4B and NS5 (Fig. 3A). This antisense RNA was in vitro synthesized and hybridized to the full-length viral RNA. Interestingly, AFM analysis of the molecules revealed the presence of both linear and circular conformations, similar to the results obtained with the short 2.3-kb molecule. Figure 3B shows representative molecules in either circular or linear conformations of the full-length viral RNA of 10.7 kb. These RNA molecules were characterized by a highly structured 5′ single strand of 6.9 kb, an extended double-stranded region with a contour length of 883 ± 5 nm, and a compact 3′ single-stranded region of 451 nucleotides. Visual inspection of images from independent sample preparations indicated that at least 25% of the molecules adopted circular conformations. The presence of RNA molecules with contour lengths shorter than the expected size suggested some RNA degradation during sample preparation. In these experiments, we counted only the molecules with the expected contour length; however, we know that partially degraded molecules lacking either 5′- or 3′-end sequences will be scored but will not be able to form circles. For this reason, it is likely that the 25% of the molecules found in circular conformation was an underestimation. Neverthe-

less, the absence of circular conformations in the control RNA, lacking the 3′-most 106 nucleotides, confirms that the amount of circular molecules observed with the genomic RNA is highly significant (data not shown).

Altogether, these results strongly support the hypothesis that specific dengue virus sequences mediate long-range RNA-RNA contacts in the viral genome.

Contacts between 5′ and 3′ CS are involved in RNA-RNA interaction. Nucleotide sequence comparisons between different flavivirus genomes indicate that the putative 5′ and 3′ CS are highly conserved in all mosquito-borne flaviviruses (Fig. 4A). In order to determine whether dengue virus 5′ and 3′CS participate in the RNA-RNA complex observed in gel shift assays, we first monitored binding of the 3′ SL probe to the unlabeled 5′ UTR-C62 RNA carrying a deletion of 5′ CS. Incubation of the probe with the 5′ UTR RNA showed no complex formation (Fig. 4B), suggesting that base pairing between 5′CS and 3′CS was necessary for the interaction. To further confirm this observation, specific mutations were incorporated into the 5′ UTR-C62 RNA molecule. Thus, we generated RNAs with 2-, 4-, 5-, and 7-nucleotide substitutions within the 11-nucleotide sequence of dengue virus 5′ CS (Fig. 4C, mutants 143, 144, 145, and 146, respectively). The WT 3′ SL probe was incubated with different concentrations of unlabeled WT and mutated 5′ UTR-C62 RNAs. The RNA binding assays indicated that a 2-nucleotide mismatch between 5′ and 3′ CS complementarity (mutant 143) was sufficient to decrease
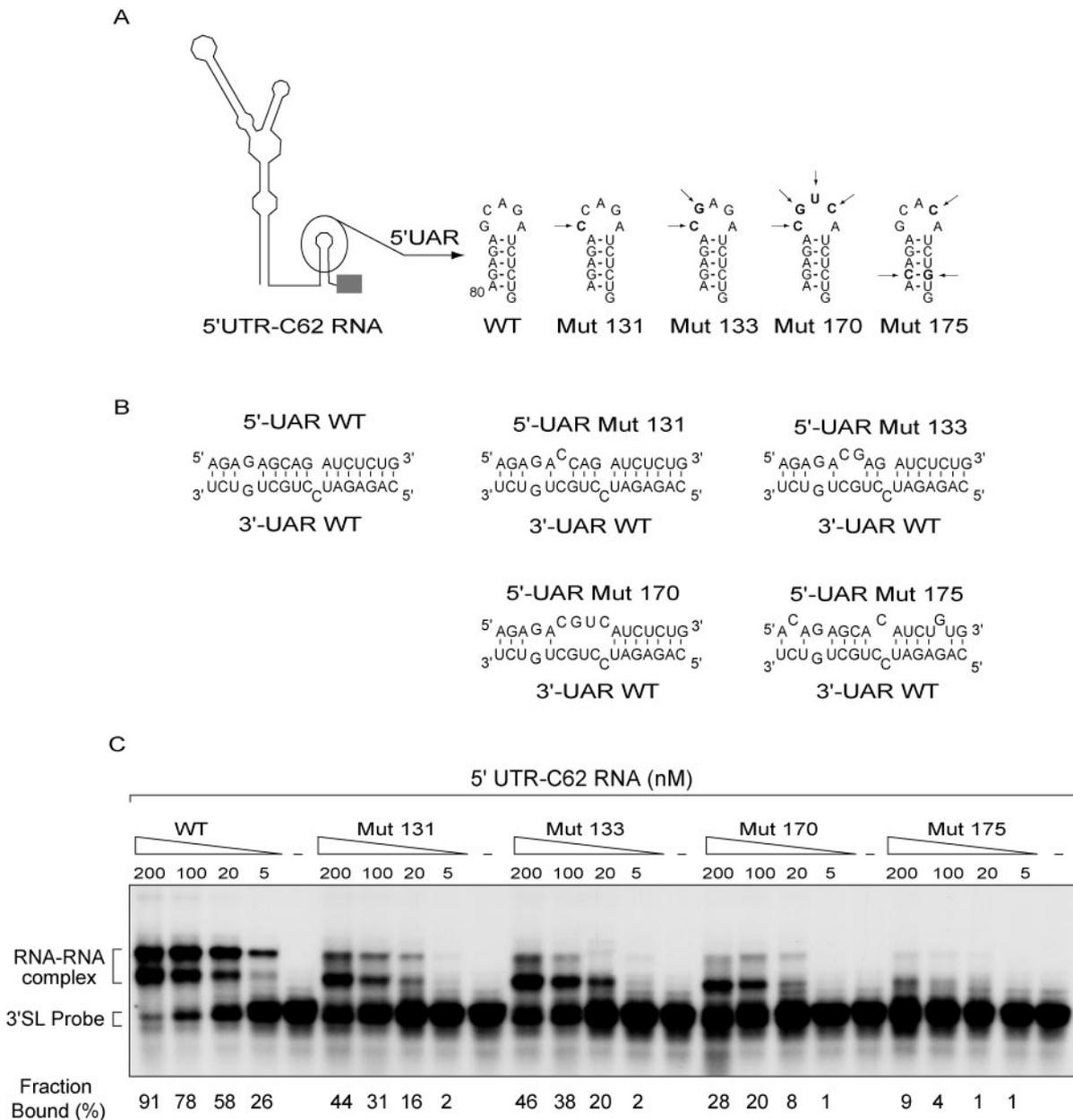
FIG. 6. Interaction between 5′ and 3′UAR sequences of dengue virus is required for RNA-RNA association. (A) Schematic representation of the predicted secondary structure of the first 160 nucleotides of dengue virus RNA. The stem-loop that contained the 16-nucleotide-long 5′ UAR is shown. The location of specific mutations (Mut) within the 5′ UAR are indicated with arrows, and the nucleotide changes are shown for mutants 131, 133, 170, and 175. (B) Base pairing between sequences corresponding to nucleotides 80 to 95 (5′ UAR) and 10642 to 10658 (3′ UAR) of the dengue virus type 2 genome are shown for the wild-type and mutated RNAs. (C) RNA mobility shift analysis showing the effect of mutations within the 5′ UAR in the 5′ UTR-C62 RNA on binding to the 3′ SL RNA. Uniformly labeled 3′ SL RNA was incubated with increasing concentrations of wild-type and mutated 5′ UTR-C62 RNAs as indicated at the top of the gel. The mobility of the 3′ SL probe and the RNA-RNA complex is indicated on the left. Quantifications of the fraction of probe bound for each concentration of the WT and mutated RNAs are also indicated at the bottom of the gel.

the RNA binding affinity more than 10-fold, changing the K_d from 8 to 100 nM (Fig. 4D). Furthermore, point mutations that included more than four base mismatches between the 5′ and 3′ CS drastically decreased RNA-RNA complex formation (Fig. 4D, mutants 144, 145, and 146). These results indicate that sequences within 5′ CS are necessary for RNA-RNA complex formation.

Mapping RNA-RNA contacts between 5′- and 3′-end sequences of dengue virus. To evaluate all possible contacts between the 5′ and 3′ ends of dengue virus RNA, we examined the predicted secondary structures of a molecule containing both the 160 nucleotides of the 5′ end (5′ UTR-C62) and the 106 nucleotides of the 3′ end of dengue virus genome by using the Mfold program (65). Two alternative folding predictions

were obtained with similar energies, and both structures showed base pairing between 5′ and 3′ CS (Fig. 5). Similar predictions were previously reported for dengue virus and other flaviviruses (38, 52, 62). In structure I, the highly conserved 3′ SL structure was retained, and the interactions between 5′ and 3′ sequences were maintained mainly by 5′-3′ CS base pairing. Structure II is very different in that the base of the 3′ SL is disrupted, allowing base pairing to occur just upstream of the initiator AUG of the 5′ UTR (Fig. 5). This second complementary sequence of 16 nucleotides bears one mismatch and one bulge. Due to its location just 5′ to the initiator AUG, we named this second putative cyclization element 5′ and 3′ UAR (upstream AUG region). To evaluate the importance of 5′-3′ UAR base pairing in RNA-RNA complex formation, we performed gel shift assays using the 5′ UTR-C62 RNAs carrying specific mutations in UAR. Because the 5′ UAR is located within a very conserved stem-loop structure (Fig. 6A), the mutations were incorporated into the loop and both sides of the stem to avoid altering the predicted stem-loop structure. Thus, we generated 5′ UTR-C62 mutants 131, 133, 175, and 170, carrying one to four substitutions, respectively (Fig. 6A). These nucleotide changes resulted in one to four mismatches within the UAR when the 5′ UTR-C62 RNA hybridizes with the 3′ SL RNA (Fig. 6B). In order to estimate the affinity between the 5′ and 3′ RNAs, the wild-type 3′ SL probe was titrated with different concentrations of each of the mutant 5′ UTR-C62 RNAs. A single G/C substitution in the 5′ UAR (mutant 131) greatly decreased the affinity for the 3′ SL RNA (Fig. 6C). Moreover, substitutions in the 5′ UAR with three or four mismatches almost abolished RNA-RNA interaction. The lack of binding of the 3′ SL RNA to RNA molecules carrying substitutions within the 5′ UAR indicates that 5′-3′ UAR interaction is involved in complex formation, suggesting that structure II (depicted in Fig. 5) is the one predicted in the RNA-RNA complex. Furthermore, these results were confirmed by AFM data, in which analysis of RNA molecules of 2.3 kb with deletions at the 3′ end including the 3′ UAR did not acquire circular conformation (data not shown).

Significance of long-range RNA-RNA interactions for viral viability. Several reports have previously demonstrated the requirement of 5′ and 3′ CS for viral replication in different flaviviruses (11, 38, 39, 42). Here, we demonstrated that in addition to 5′-3′ CS complementarity, a second RNA region present at the 5′ and 3′ UTR of dengue virus (named 5′ and 3′ UAR) is required for RNA-RNA complex formation (see structure II in Fig. 5). Thus, to further substantiate the notion that genome circularization is indeed required for viral replication, we asked whether 5′-3′ UAR complementarity is necessary during the viral life cycle. To this end, we constructed recombinant dengue virus RNAs carrying substitutions in the 5′ or 3′ UAR and in both 5′-3′ UAR which will disrupt or reconstitute the 5′-3′ complementarity, respectively. The 5′ UAR mutant contained three nucleotide substitutions (80-AC AAGACAC AUCUGUG [the substitutions are underlined]) (Fig. 7A, DV-5′UAR 175). This mutation was shown to abolish RNA-RNA complex formation in the RNA binding assay (Fig. 6, mutant 175). The recombinant viral RNA carrying the mutation at the 3′ end contained four substitutions (three substitutions in the 3′ UAR [underlined] [10634-CACAGAUCGU GCUGUGU] and one G/C substitution at position 10718).
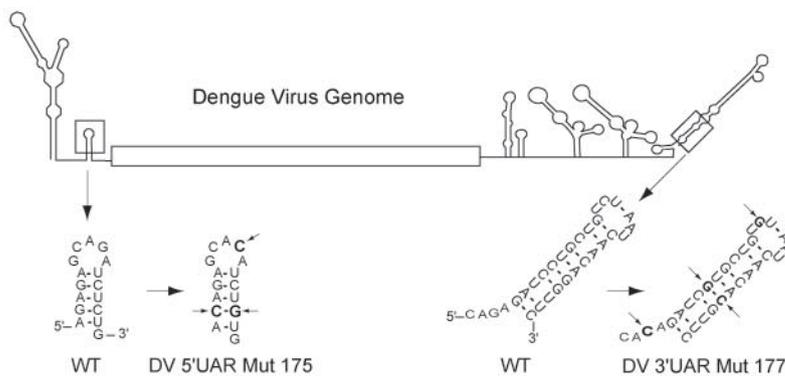
The three substitutions in the UAR were designed to restore complementarity with mutant 5′UAR 175, and the fourth substitution was designed to maintain the predicted structure of the 3′ SL (Fig. 7A, DV-3′UAR 177). We also generated the recombinant dengue virus RNA containing both mutations at the 5′ and 3′ ends in a single RNA (DV-5′-3′UAR 175-177) simultaneously.

In order to confirm that the mutations designed at the 5′ and 3′ UAR based on RNA-folding predictions indeed restore RNA-RNA interaction, we performed gel shift analysis with a 3′ SL probe carrying the mutation in the 3′ UAR (3′ SL 177). This probe was incubated with unlabeled WT or mutated 5′ UTR-C62 RNA carrying mutation 175. The RNA binding assays indicated that the 3′ SL 177 probe interacted very weakly with the WT 5′ UTR-C62 RNA, but RNA-RNA binding affinity was greatly increased when mutant 175 was used as the unlabeled RNA (Fig. 7B, lanes 10 to 17). Therefore, we concluded that combining the mutations in the 5′ and 3′ UAR restores RNA-RNA interaction. Titrations of the probes 3′ SL WT and 3′ SL 177 with different concentrations of unlabeled RNAs indicated that the affinity between the two mutant RNAs is similar to that observed with the two WT RNAs (Fig. 7B, compare lanes 1 to 4 with lanes 10 to 13).
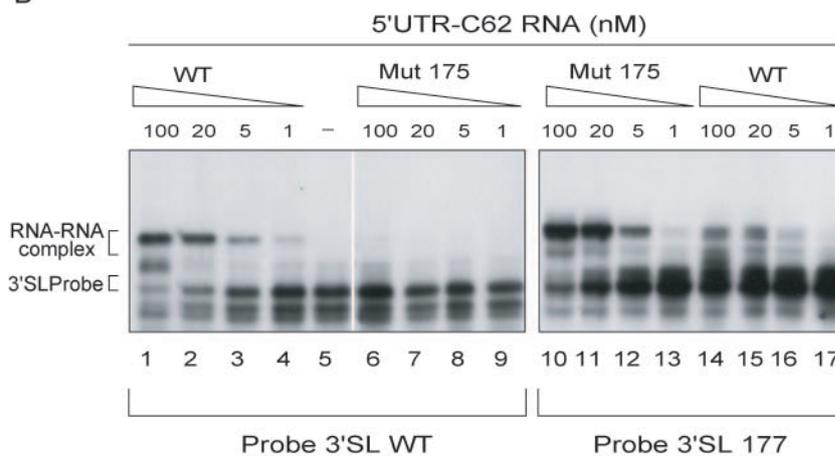
Next, we in vitro transcribed and transfected into BHK cells full-length dengue virus RNAs corresponding to the WT and mutants DV-5′UAR 175, DV-3′UAR 177, and DV-5′-3′ UAR 175-177. Initially, the infectivity of the RNAs was assessed by IFA for dengue virus antigens in transfected cells by using murine anti-dengue virus type 2 antibodies. The cells transfected with DV-5′UAR 175 and DV-3′UAR 177 RNAs were negative at 3, 6, 9, 12, 15, 18, and 21 days (Fig. 7C). For this experiment, cells were reseeded at 3-day intervals. In contrast, when the cells were transfected with the double mutant DV-5′3′UAR 175-177 RNA, the IFA was positive at day 3 after transfection, and about 10% of the monolayer was positive at day 9 (Fig. 7C). The WT RNA-transfected cells were positive for dengue virus antigens by IFA by 24 h, and nearly 100% of cells in the monolayer were positive at day 4. This result indicates that mutations in both the 5′ and 3′ UAR that reconstitute RNA-RNA interactions rescue the lethal phenotype of substitutions either at the 5′ or the 3′ UAR sequences. Assuming that the efficiency of transfection of cells with WT and mutant RNAs was similar, this result indicates that the DV 5′-3′UAR 175-177 mutant virus did replicate in the transfected cells but that replication was markedly impaired in comparison with that of the WT virus.

To confirm these results, we searched for infectious dengue virus particles after transfections. The media from cells transfected with WT and mutated RNAs were collected after 3, 6, 9, 12, 15, 18, and 21 days and used for plaque assays in BHK cells. Infectious particles were not recovered for the single mutants at the 5′ and 3′ UAR. In contrast, the double-mutant RNA yielded viral particles with a small-plaque phenotype in comparison to that of WT virus (Fig. 7D). The plaque size observed after 9 days of infection of BHK cells with the mutant virus collected after 9, 12, 15, 18, and 21 days after transfection remained small (2 mm compared with 4 mm of the WT). Furthermore, we analyzed whether nucleotide changes in the mutant viruses occurred during virus cultivation. To this end, RNA was extracted from viruses collected in the media from
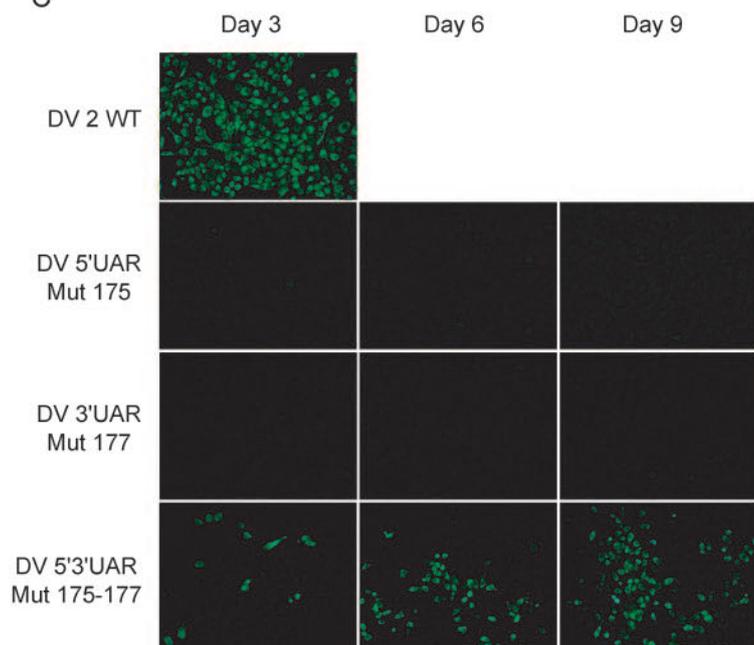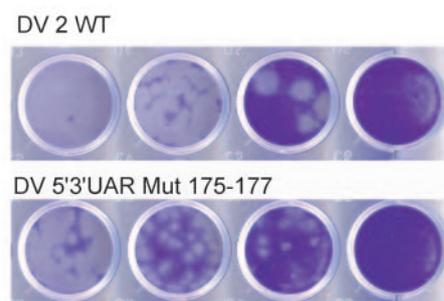
A

B

5'UTR-C62 RNA (nM)

Probe 3'SL WT

Probe 3'SL 177

C

| | Day 3 | Day 6 | Day 9 |

DV 2 WT

DV 5'UAR Mut 175

DV 3'UAR Mut 177

DV 5'3'UAR Mut 175-177

D

DV 2 WT

DV 5'3'UAR Mut 175-177

transfected cells at different times and used for RT-PCR. Sequencing analysis of the cDNAs revealed that the original substitutions in the double-mutant virus were retained. These results were reproduced in three independent experiments.

Taken together, these results indicate that point mutations in either the 5′ or the 3′ UAR were lethal and that reconstitution of the RNA-RNA complementarity between these sequences was essential for viral viability. In addition, the impaired replication of the virus DV-5′3′UAR 175-177 strongly suggested that UAR nucleotide sequence and/or RNA structures involving the UAR at the 5′ UTR and the 3′ SL is required for efficient dengue virus replication.

DISCUSSION

In this study, we provide direct evidence for long-range RNA-RNA interactions in the dengue virus genome. Using AFM, we visualized individual RNA molecules in circular conformations. Novel complementary sequences present at the 5′ and 3′ ends of the viral genome were identified as determinants for RNA-RNA contacts. More importantly, analysis of recombinant dengue viruses indicate that complementarity between these sequences is essential for viral replication. The data presented here, together with previous reports, support the notion that communication between 5′ and 3′ ends of RNA molecules could be a common feature of both host mRNAs and viral RNA genomes (6, 30–32, 59).

AFM is a powerful technique that has been shown to be useful for studying conformations of DNA, structures of DNA-protein complexes, and motion of enzymatic reactions (such as transcription) at the single-molecule level (9, 24, 26, 28, 29, 36, 45). In contrast, fewer studies analyzing biologically relevant RNA molecules have been reported (1, 2, 53, 59). Here, we used AFM to investigate long-range RNA-RNA interactions between conserved RNA elements present in the genome of mosquito-borne flaviviruses. RNA molecules of 2.3 kb carrying dengue virus sequences at the 5′ and 3′ ends acquire circular conformations (Fig. 2), while control RNA with deletions of specific dengue virus sequences at the 3′ end was unable to form circles (Table 1). Similar results were obtained using the full-length dengue virus RNA of 10.7 kb (Fig. 3). The statistically significant amount of circular molecules found in the samples indicated that the affinity between the RNA elements

present at the ends of the dengue virus genome was sufficient for RNA circularization. Analysis of RNA-RNA complexes formed in vitro together with AFM data indicated that at least two pairs of complementary sequences were necessary for RNA-RNA interactions. We demonstrated that base pairing between the 5′ and 3′ CS alone was not sufficient for in vitro RNA-RNA complex formation. A second complementary sequence present at the 5′ end just upstream of the initiator AUG and at the 3′ end within the 3′ SL (5′ and 3′ UAR) was also required. Single nucleotide changes within the CS or UAR showed a large effect on the affinity of the 5′ and 3′ RNAs (Fig. 4 and 6), suggesting that interactions between the two pairs of complementary sequences are important to stabilize the RNA-RNA association. However, the absolute requirement of Mg^{2+} for complex formation strongly suggests that 5′-3′ association also involves tertiary structures in the RNA.

The 5′ and 3′ CS are 10 or more contiguous nucleotides that complement perfectly in all mosquito-borne flaviviruses. Sequence analysis indicates that at least eight of these nucleotides are identical in these viruses (Fig. 4A), suggesting that even though coevolution of the two complementary sequences could occur, there must be a growth advantage to preserve the nucleotide sequences. A number of reports using mutational analysis in different flaviviruses have demonstrated the requirement of 5′ and 3′ CS for viral replication (11, 38, 39, 42). In contrast, a possible role of 5′ and 3′ UAR sequences in viral replication was not previously inspected. Here, we show that specific substitutions within the 5′ or 3′ UAR in the context of infectious dengue virus type 2 yielded no viable viruses. Importantly, mutations at the 5′ and 3′ UAR that restore complementarity were sufficient to rescue viral replication, demonstrating that base pairing of 5′-3′ UAR provides an essential element for viral viability. In addition, the small-plaque phenotype observed with the mutant virus suggests that the nucleotide sequence of the 5′ and 3′ UAR is required for efficient viral replication. Because the cyclization motives are widely conserved among flaviviruses, the results presented here could be extrapolated to other members of this genus.

Roles of RNA cyclization during viral replication. It is a common notion that RNA elements at the 5′ end of viral RNAs modulate the efficiency of translation initiation, while elements at the 3′ end recruit the replication machinery to initiate negative-strand RNA synthesis. This view is now

FIG. 7. Specific mutations within the 5′ or 3′ UAR abolish viral replication, while reconstitution of 5′-3′ UAR complementarity restores the viral function. (A) Schematic representation of the dengue virus genome showing the predicted secondary structure of the RNA elements containing 5′ and 3′UAR (shown in boxes). Nucleotide sequences of wild-type and mutant (Mut) DV 5′UAR 175 and DV 3′UAR 177 are shown. Mutations are highlighted and marked by arrows. Mutations were designed to maintain the secondary structure of the stem-loop upstream of the initiator AUG at the 5′ end and the stem of the 3′ SL at the 3′ end of the genome. (B) RNA mobility shift assays showing that reconstitution of 5′-3′ UAR complementarity restores RNA-RNA complex formation. Two different 3′ SL probes, WT and 177, were incubated with decreasing concentrations of WT or mutant 175 unlabeled 5′ UTR-C62 RNAs as indicated in each case on the top of the gel. The mobility of the probe and the RNA-RNA complex is indicated on the left. (C) Expression of dengue virus proteins in cells transfected with wild-type and mutated viral RNAs was monitored by IFA using dengue virus type 2 murine hyperimmune ascitic fluid. BHK cells grown in 60-mm culture plates were transfected with 3 μg of in vitro-transcribed full-length dengue virus RNA. Cells were trypsinized on days 3, 6, and 9 after transfection and reseeded to a coverslip for IFA analysis. Transfection of RNA with mutations only at the 5′ or 3′ UAR (DV 5′UAR 175 and DV 3′UAR 177, respectively) did not show immunofluorescence, while the double mutant DV 5′3′UAR 175–177 showed positive IFA at day 3. Cells transfected with wild-type dengue virus RNA after day 4 are not shown because they were dead due to viral infection. (D) Comparison of plaque size formed by dengue virus wild type (DV2 WT) and double mutant that reconstitute 5′-3′ UAR complementarity (DV 5′3′UAR 175–177). Serial dilutions of DV2 WT and DV 5′3′UAR 175–177 (obtained from supernatants of cells 9 days after transfection) were used to infect a monolayer of BHK cells. The monolayer was stained 9 days after infection.

changing, as accumulating evidence indicates that the roles of both the 5′ and 3′ ends functionally overlap. For instance, sequences at the 5′ end of poliovirus, Sindbis virus, and alfalfa mosaic virus are essential for negative-strand synthesis at the 3′ end (16–19, 21, 55), while *cis*-acting elements at the 3′ UTR of viral genomes have been shown to modulate the efficiency of translation initiation at the 5′ end (3, 44, 57, 58). In dengue virus, it was proposed that sequences within the 5′ CS annealed to the 3′ CS to provide the recognition signals for RNA synthesis by the viral NS5 polymerase (62, 63). Cyclization of the dengue virus genome is likely to induce changes both upstream of the initiator AUG and within the structure of the very conserved 3′ SL (Fig. 5). Because these two elements are *cis*-acting signals for translation and RNA synthesis, it is possible that changes in the RNA conformation could modulate these steps of viral replication. Taken together, we hypothesize that bringing the initiation sites for translation and RNA synthesis physically together provides a strategy to coordinate both processes. Further studies using dengue virus replicons expressing a reporter gene are under way in our laboratory to dissect the role(s) of circular conformations of the RNA in each step of the viral life cycle.

In the present study, we observed RNA-RNA interactions in the absence of proteins. However, it is likely that cellular or viral proteins modulate the formation or stabilization of circular or linear RNAs in vivo. In fact, it has been proposed that the viral protease NS3 binds to dengue virus 3′ SL (12), the cellular protein EF-1α interacts with several flavivirus 3′ SLs (5, 13), and the cellular La protein binds both 5′ and 3′ UTR elements (20). In the case of Japanese encephalitis virus, both NS3 and NS5 proteins bind cooperatively to the 3′ SL (10). Because the cyclization 3′ UAR sequences are located within the 3′ SL structure, binding of cellular or viral proteins to this RNA element could disrupt or enhance cyclization of the viral genome in the infected cell.

Clearly, secondary and tertiary structures of viral RNAs serve highly conserved functions in viral replication. In addition, these structures of the RNA could change during the viral life cycle, adopting different conformations during translation, RNA synthesis, and encapsidation. Therefore, further analysis of RNA conformations acquired during these processes will help to clarify molecular details of viral replication.

REFERENCES

1. **Andersen, E. S., S. A. Contera, B. Knudsen, C. K. Damgaard, F. Besenbacher, and J. Kjems.** 2004. Role of the trans-activation response element in dimerization of HIV-1 RNA. J. Biol. Chem. **279:**22243–22249.
2. **Andreev, I. A., S. H. Kim, N. O. Kalinina, D. V. Rakitina, A. G. Fitzgerald, P. Palukaitis, and M. E. Taliansky.** 2004. Molecular interactions between a plant virus movement protein and RNA: force spectroscopy investigation. J. Mol. Biol. **339:**1041–1047.
3. **Barends, S., H. H. Bink, S. H. van den Worm, C. W. Pleij, and B. Kraal.** 2003. Entrapping ribosomes for viral translation: tRNA mimicry as a molecular Trojan horse. Cell **112:**123–129.
4. **Barton, D. J., B. J. O'Donnell, and J. B. Flanegan.** 2001. 5′ cloverleaf in poliovirus RNA is a cis-acting replication element required for negative-strand synthesis. EMBO J. **20:**1439–1448.
5. **Blackwell, J. L., and M. A. Brinton.** 1997. Translation elongation factor-1 alpha interacts with the 3′ stem-loop region of West Nile virus genomic RNA. J. Virol. **71:**6433–6444.
6. **Blumenthal, T., and G. G. Carmichael.** 1979. RNA replication: function and structure of Qbeta-replicase. Annu. Rev. Biochem. **48:**525–548.
7. **Bonin, M., J. Oberstrass, N. Lukacs, K. Ewert, E. Oesterschulze, R. Kassing, and W. Nellen.** 2000. Determination of preferential binding sites for anti-dsRNA antibodies on double-stranded RNA by scanning force microscopy. RNA **6:**563–570.
8. **Brinton, M. A., A. V. Fernandez, and J. H. Dispoto.** 1986. The 3′-nucleotides of flavivirus genomic RNA form a conserved secondary structure. Virology **153:**113–121.
9. **Bustamante, C., and C. Rivetti.** 1996. Visualizing protein-nucleic acid interactions on a large scale with the scanning force microscope. Annu. Rev. Biophys. Biomol. Struct. **25:**395–429.
10. **Chen, C. J., M. D. Kuo, L. J. Chien, S. L. Hsu, Y. M. Wang, and J. H. Lin.** 1997. RNA-protein interactions: involvement of NS3, NS5, and 3′ noncoding regions of Japanese encephalitis virus genomic RNA. J. Virol. **71:**3466–3473.
11. **Corver, J., E. Lenches, K. Smith, R. A. Robison, T. Sando, E. G. Strauss, and J. H. Strauss.** 2003. Fine mapping of a *cis*-acting sequence element in yellow fever virus RNA that is required for RNA replication and cyclization. J. Virol. **77:**2265–2270.
12. **Cui, T., R. J. Sugrue, Q. Xu, A. K. Lee, Y. C. Chan, and J. Fu.** 1998. Recombinant dengue virus type 1 NS3 protein exhibits specific viral RNA binding and NTPase activity regulated by the NS5 protein. Virology **246:**409–417.
13. **De Nova-Ocampo, M., N. Villegas-Sepulveda, and R. M. del Angel.** 2002. Translation elongation factor-1alpha, La, and PTB interact with the 3′ untranslated region of dengue 4 virus RNA. Virology **295:**337–347.
14. **Fang, X., T. Pan, and T. R. Sosnick.** 1999. A thermodynamic framework and cooperativity in the tertiary folding of a Mg2+-dependent ribozyme. Biochemistry **38:**16840–16846.
15. **Frey, T. K., D. L. Gard, and J. H. Strauss.** 1979. Biophysical studies on circle formation by Sindbis virus 49 S RNA. J. Mol. Biol. **132:**1–18.
16. **Frolov, I., R. Hardy, and C. M. Rice.** 2001. *Cis*-acting RNA elements at the 5′ end of Sindbis virus genome RNA regulate minus- and plus-strand RNA synthesis. RNA **7:**1638–1651.
17. **Gamarnik, A. V., and R. Andino.** 2000. Interactions of viral protein 3CD and poly(rC) binding protein with the 5′ untranslated region of the poliovirus genome. J. Virol. **74:**2219–2226.
18. **Gamarnik, A. V., and R. Andino.** 1998. Switch from translation to RNA replication in a positive-stranded RNA virus. Genes Dev. **12:**2293–2304.
19. **Gamarnik, A. V., and R. Andino.** 1997. Two functional complexes formed by KH domain containing proteins with the 5′ noncoding region of poliovirus RNA. RNA **3:**882–892.
20. **Garcia-Montalvo, B. M., F. Medina, and R. M. del Angel.** 2004. La protein binds to NS5 and NS3 and to the 5′ and 3′ ends of dengue 4 virus RNA. Virus Res. **102:**141–150.
21. **Gorchakov, R., R. Hardy, C. M. Rice, and I. Frolov.** 2004. Selection of functional 5′ *cis*-acting elements promoting efficient Sindbis virus genome replication. J. Virol. **78:**61–75.
22. **Guo, L., E. M. Allen, and W. A. Miller.** 2001. Base-pairing between untranslated regions facilitates translation of uncapped, nonpolyadenylated viral RNA. Mol. Cell **7:**1103–1109.
23. **Hahn, C. S., Y. S. Hahn, C. M. Rice, E. Lee, L. Dalgarno, E. G. Strauss, and J. H. Strauss.** 1987. Conserved elements in the 3′ untranslated region of flavivirus RNAs and potential cyclization sequences. J. Mol. Biol. **198:**33–41.
24. **Hansma, H. G., K. Kasuya, and E. Oroudjev.** 2004. Atomic force microscopy imaging and pulling of nucleic acids. Curr. Opin. Struct. Biol. **14:**380–385.
25. **Hansma, H. G., K. J. Kim, D. E. Laney, R. A. Garcia, M. Argaman, M. J. Allen, and S. M. Parsons.** 1997. Properties of biomolecules measured from atomic force microscope images: a review. J. Struct. Biol. **119:**99–108.
26. **Hansma, H. G., and D. E. Laney.** 1996. DNA binding to mica correlates with cationic radius: assay by atomic force microscopy. Biophys. J. **70:**1933–1939.
27. **Hansma, H. G., I. Revenko, K. Kim, and D. E. Laney.** 1996. Atomic force microscopy of long and short double-stranded, single-stranded and triple-stranded nucleic acids. Nucleic Acids Res. **24:**713–720.
28. **Hansma, H. G., J. Vesenka, C. Siegerist, G. Kelderman, H. Morrett, R. L. Sinsheimer, V. Elings, C. Bustamante, and P. K. Hansma.** 1992. Reproducible imaging and dissection of plasmid DNA under liquid with the atomic force microscope. Science **256:**1180–1184.
29. **Henn, A., O. Medalia, S. P. Shi, M. Steinberg, F. Franceschi, and I. Sagi.** 2001. Visualization of unwinding activity of duplex RNA by DbpA, a DEAD box helicase, at single-molecule resolution by atomic force microscopy. Proc. Natl. Acad. Sci. USA **98:**5007–5012.
30. **Herold, J., and R. Andino.** 2001. Poliovirus RNA replication requires genome circularization through a protein-protein bridge. Mol. Cell **7:**581–591.

31. **Hewlett, M. J., R. F. Pettersson, and D. Baltimore.** 1977. Circular forms of Uukuniemi virion RNA: an electron microscopic study. J. Virol. **21:**1085–1093.
32. **Hsu, M. T., J. D. Parvin, S. Gupta, M. Krystal, and P. Palese.** 1987. Genomic RNAs of influenza viruses are held in a circular conformation in virions and in infected cells by a terminal panhandle. Proc. Natl. Acad. Sci. USA **84:** 8140–8144.
33. **Isken, O., C. W. Grassmann, R. T. Sarisky, M. Kann, S. Zhang, F. Grosse, P. N. Kao, and S. E. Behrens.** 2003. Members of the NF90/NFAR protein group are involved in the life cycle of a positive-strand RNA virus. EMBO J. **22:**5655–5665.
34. **Jun, S., J. Herrick, A. Bensimon, and J. Bechhoefer.** 2004. Persistence length of chromatin determines origin spacing in Xenopus early-embryo DNA replication: quantitative comparisons between theory and experiment. Cell Cycle **3:**223–229.
35. **Kapahnke, R., W. Rappold, U. Desselberger, and D. Riesner.** 1986. The stiffness of dsRNA: hydrodynamic studies on fluorescence-labelled RNA segments of bovine rotavirus. Nucleic Acids Res. **14:**3215–3228.
36. **Kasas, S., N. H. Thomson, B. L. Smith, H. G. Hansma, X. Zhu, M. Guthold, C. Bustamante, E. T. Kool, M. Kashlev, and P. K. Hansma.** 1997. Escherichia coli RNA polymerase activity observed using atomic force microscopy. Biochemistry **36:**461–468.
37. **Khromykh, A. A., N. Kondratieva, J. Y. Sgro, A. Palmenberg, and E. G. Westaway.** 2003. Significance in replication of the terminal nucleotides of the flavivirus genome. J. Virol. **77:**10623–10629.
38. **Khromykh, A. A., H. Meka, K. J. Guyatt, and E. G. Westaway.** 2001. Essential role of cyclization sequences in flavivirus RNA replication. J. Virol. **75:**6719–6728.
39. **Khromykh, B. L., and E. G. Westaway.** 1997. Subgenomic replicons of the flavivirus Kunjin: construction and applications. J. Virol. **71:**1497–1505.
40. **Kinney, R. M., S. Butrapet, G. J. Chang, K. R. Tsuchiya, J. T. Roehrig, N. Bhamarapravati, and D. J. Gubler.** 1997. Construction of infectious cDNA clones for dengue 2 virus: strain 16681 and its attenuated vaccine derivative, strain PDK-53. Virology **230:**300–308.
41. **Markoff, L.** 2003. 5′ and 3′ noncoding regions in flavivirus RNA. Adv. Virus Res. **59:**177–228.
42. **Men, R., M. Bray, D. Clark, R. M. Chanock, and C. J. Lai.** 1996. Dengue type 4 virus mutants containing deletions in the 3′ noncoding region of the RNA genome: analysis of growth restriction in cell culture and altered viremia pattern and immunogenicity in rhesus monkeys. J. Virol. **70:**3930–3937.
43. **Misra, V. K., and D. E. Draper.** 2002. The linkage between magnesium binding and RNA folding. J. Mol. Biol. **317:**507–521.
44. **Neeleman, L., R. C. Olsthoorn, H. J. Linthorst, and J. F. Bol.** 2001. Translation of a nonpolyadenylated viral RNA is enhanced by binding of viral coat protein or polyadenylation of the RNA. Proc. Natl. Acad. Sci. USA **98:** 14286–14291.
45. **Pietrasanta, L. I., D. Thrower, W. Hsieh, S. Rao, O. Stemmann, J. Lechner, J. Carbon, and H. Hansma.** 1999. Probing the Saccharomyces cerevisiae centromeric DNA (CEN DNA)-binding factor 3 (CBF3) kinetochore complex by using atomic force microscopy. Proc. Natl. Acad. Sci. USA **96:**3757–3762.
46. **Piron, M., P. Vende, J. Cohen, and D. Poncet.** 1998. Rotavirus RNA-binding protein NSP3 interacts with eIF4GI and evicts the poly(A) binding protein from eIF4F. EMBO J. **17:**5811–5821.
47. **Proutski, V., E. A. Gould, and E. C. Holmes.** 1997. Secondary structure of the 3′ untranslated region of flaviviruses: similarities and differences. Nucleic Acids Res. **25:**1194–1202.
48. **Rauscher, S., C. Flamm, C. W. Mandl, F. X. Heinz, and P. F. Stadler.** 1997. Secondary structure of the 3′-noncoding region of flavivirus genomes: comparative analysis of base pairing probabilities. RNA **3:**779–791.
49. **Rice, C.** 2001. Flaviviridae: the viruses and their replication, p.991–1044. *In* D. M. Knipe, P. M. Howley, D. E. Griffin, R. A. Lamb, M. A. Martin, B. Roizman, and S. E. Straus (ed.), Fields virology, 4th ed., vol. 1. Lippincott-Raven Publishers, Philadelphia, Pa.
50. **Saenger, W.** 1984. Principles of nucleic acid structures. Springer Verlag, New York, N.Y.
51. **Shurtleff, A. C., D. W. Beasley, J. J. Chen, H. Ni, M. T. Suderman, H. Wang, R. Xu, E. Wang, S. C. Weaver, D. M. Watts, K. L. Russell, and A. D. Barrett.** 2001. Genetic variation in the 3′ non-coding region of dengue viruses. Virology **281:**75–87.
52. **Thurner, C., C. Witwer, I. L. Hofacker, and P. F. Stadler.** 2004. Conserved RNA secondary structures in Flaviviridae genomes. J. Gen. Virol. **85:**1113–1124.
53. **Trottier, M., Y. Mat-Arip, C. Zhang, C. Chen, S. Sheng, Z. Shao, and P. Guo.** 2000. Probing the structure of monomers and dimers of the bacterial virus phi29 hexamer RNA complex by chemical modification. RNA **6:**1257–1266.
54. **Vende, P., M. Piron, N. Castagne, and D. Poncet.** 2000. Efficient translation of rotavirus mRNA requires simultaneous interaction of NSP3 with the eukaryotic translation initiation factor eIF4G and the mRNA 3′ end. J. Virol. **74:**7064–7071.
55. **Vlot, A. C., and J. F. Bol.** 2003. The 5′ untranslated region of alfalfa mosaic virus RNA 1 is involved in negative-strand RNA synthesis. J. Virol. **77:** 11284–11289.
56. **Walter, B. L., T. B. Parsley, E. Ehrenfeld, and B. L. Semler.** 2002. Distinct poly(rC) binding protein KH domain determinants for poliovirus translation initiation and viral RNA replication. J. Virol. **76:**12008–12022.
57. **Wang, S., K. S. Browning, and W. A. Miller.** 1997. A viral sequence in the 3′-untranslated region mimics a 5′ cap in facilitating translation of uncapped mRNA. EMBO J. **16:**4107–4116.
58. **Wang, S., L. Guo, E. Allen, and W. A. Miller.** 1999. A potential mechanism for selective control of cap-independent translation by a viral RNA sequence in cis and in trans. RNA **5:**728–738.
59. **Wells, S. E., P. E. Hillner, R. D. Vale, and A. B. Sachs.** 1998. Circularization of mRNA by eukaryotic translation initiation factors. Mol. Cell **2:**135–140.
60. **World Health Organization.** 2002. Disease outbreak news. World Health Organization, Geneva, Switzerland.
61. **Yamakawa, H.** 1997. Helical wormlike chains in polymer solutions. Springer, Berlin, Germany.
62. **You, S., B. Falgout, L. Markoff, and R. Padmanabhan.** 2001. In vitro RNA synthesis from exogenous dengue viral RNA templates requires long range interactions between 5′- and 3′-terminal regions that influence RNA structure. J. Biol. Chem. **276:**15581–15591.
63. **You, S., and R. Padmanabhan.** 1999. A novel in vitro replication system for dengue virus. Initiation of RNA synthesis at the 3′-end of exogenous viral RNA templates requires 5′- and 3′-terminal complementary sequence motifs of the viral RNA. J. Biol. Chem. **274:**33714–33722.
64. **Zeng, L., B. Falgout, and L. Markoff.** 1998. Identification of specific nucleotide sequences within the conserved 3′-SL in the dengue type 2 virus genome required for replication. J. Virol. **72:**7510–7522.
65. **Zuker, M.** 2003. Mfold web server for nucleic acid folding and hybridization prediction. Nucleic Acids Res. **31:**3406–3415.